Available online at www.sciencedirect.com
ScienceDirect
Journal of Sound and Vibration 313 (2008) 433–448
JOURNAL OF SOUND AND VIBRATION
www.elsevier.com/locate/jsvi

Turbofan duct liner design/optimization: A statistical method

Gabriel Zlavog, Walter Eversman*

Department of Mechanical and Aerospace Engineering, University of Missouri-Rolla, 202 Mechanical Engineering Building, 1870 Miner Circle, Rolla, MO 65409-0050, USA

Received 19 May 2005; received in revised form 14 September 2007; accepted 20 September 2007
Available online 14 March 2008

Abstract

A statistical method for design optimization of acoustic liners for turbofan inlets is developed. This approach is motivated by the observation that the performance of acoustic treatment is dependent on the details of the source. For broadband noise the source is inherently random and for tonal noise in most cases the precise source structure is uncertain. The source is defined by many trials of randomly selected modal powers and modal phases, and with an efficient model of duct propagation, statistical descriptions of realized attenuation are generated with repeatable mean and standard deviation. The method is demonstrated for optimization of acoustic treatment for tonal noise, for broadband noise at specific frequencies, and for spectral attenuation. Comparisons of optimized linings with linings developed in a published experimental program are used to investigate performance predictions.

1. Introduction

Noise reduction obtained by acoustical treatment in turbofan inlets and exhaust ducts is critical in satisfying aircraft noise regulations. Research efforts have focused on the development of numerical and analytical models of sound transmission through lined aircraft engine nacelles with the ultimate purpose of prediction of acoustic lining performance and the design of optimum linings.

Early endeavors in determination of optimal acoustic lining performance are reviewed in a paper by Lester and Posey [1]. They were generally based on optimization of attenuation of acoustic modes in uniform ducts. Certain simplifying assumptions about the modal source were made. Contemporary methods for finding the most favorable linings are exemplified by multi-element lining optimization (MELO), which is a modal attenuation code [2], and CDUCT, a parabolized approximation of the convected wave equation [3].

MELO is an infinite duct program that considers uniform ducts with mean flow with a boundary layer. It does not account for varying geometry. The source description is based on equal modal power. This assumption was considered appropriate for approach and cut-back flight conditions that are dominated by broad-band noise. Dyer [4] showed that for high frequencies, statistically averaged acoustic random power in hard wall ducts can be obtained by assuming equal partition of energy among all cut-on modes. In the description of the code MELO it is not explicitly stated how modal phases were chosen. It has been shown in

*Corresponding author. Tel.: +1 573 341 4670; fax: +1 573 341 4607.
E-mail address: eversman@umr.edu (W. Eversman).

0022-460X/$ - see front matter © 2007 Elsevier Ltd. All rights reserved.
doi:10.1016/j.jsv.2007.09.057

Ref. [5] that with an equal modal power assumption, transmitted power in a lined duct is strongly dependent on the choice of modal phase.

Zlavog and Eversman [6,7] show with numerical experimentation and with statistical analysis that total transmitted power in a lined duct has a Gaussian distribution when all incident angular and radial modes at a given frequency are considered. In case of a single angular mode, transmitted power is Gaussian distributed in case of random radial modal power with fixed phase, and it is non-Gaussian over many trials of random phase with fixed modal power distribution.

The CDUCT parabolized convected wave equation code [3] models a three-dimensional non-uniform duct with mean flow. For well propagating modes (high cut-ff ratio) forward propagation is modeled accurately; however, fidelity is reduced for near cut-off modes. There is no back scattering and reflections are not modeled. It is not known how well forward scattering is modeled. CDUCT has the advantage of being fully three dimensional in the geometry and propagation model, but it is without a consistent model of radiation to the far field. As described in Ref. [3] the source model is a plane wave, however, evolutions of the code undoubtedly consider multi-modal input.

Until recently, the finite element method was considered to be too computationally demanding for rapid acoustic treatment design procedures. However, improvements in computer memory and CPU performance, as well as enhanced codes with parallel processing capabilities now allow finite element methods to engage optimization tasks. A step in this direction was described by Lafronza et al. [8]. They used a segmented duct model with reflection free termination based on axially symmetric duct acoustic modes computed with a finite element approach. The study presented here extends upon this by using a full finite element model for propagation in a non-uniform axially symmetric duct with reflection free termination and a statistical description of the source.

In this paper the problem of the determination of optimal acoustic liners for non-uniform axi-symmetric ducts with flow, for several design objectives is discussed. Numerical optimization algorithms are applied to an objective function representing acoustic power attenuation obtained as a result of a finite element propagation model [9,10] that discretizes the acoustic field in the duct. The lining does not necessarily extend the full length of the duct and can be multi-sectional, each section with its own impedance, such that modal scattering at impedance changes is taken into account. Mean flow, specified at the source plane, is compressible potential flow, affected by the geometry of the duct. Modal magnitudes, as well as their phases are required to be specified at the source. The eigen-problem developed from the acoustic field equations is the starting point for calculating the acoustic modes at the source and termination planes. The calculated transmitted and reflected modal amplitudes, as well as the input incident ones are used to calculate acoustic power according to Morfey's formulation [11]. Transmitted power or power transmission loss represents the outcome of the finite element propagation model.

The finite element method of calculating acoustic power attenuation is joined with a constrained numerical global optimization procedure with normalized resistance (always positive) and reactance as variables. In the case of optimizing the overall attenuation for a full range of frequencies in a broad spectrum, the optimized variables are the perforate fraction open area and honeycomb depth. The optimal lining has reactance that varies with frequency for a fixed optimum fraction open area and backing depth.

A downhill simplex method [12] with restart from different initial values feature (to insure global optimum) was tested in the optimization process. Also, a simulated annealing method was tried concurrently to evaluate performance. The downhill simplex method typically took a smaller number of iterations than the simulated annealing method to converge to the optimum.

In some cases, acoustic performance for linings consisting of two or three sections with different impedances has been compared with the performance of linings with the same overall length, but with a single impedance. Lining placement with respect to the source can also be a design parameter in attenuation performance [5], but is not considered in the present study.

A new approach for representation of statistically defined modal sources is used in this study. This approach proposes random incident modal powers and random modal phases. It has been shown in Ref. [5] that consideration of a relatively large number of random modal sets (e.g., 1000) produces a repeatable statistical description of attenuation in terms of mean and standard deviation. The mean attenuation can be maximized in the optimization process. A more cautious approach, only briefly touched in this paper, could maximize the

lowest attenuation in the attenuation range. The method of random modal input is applicable especially to broadband noise, characterized by many circumferential and radial propagating modes. It is applicable also to tonal noise for which the circumferential mode is known, but the explicit description of the radial modal content is uncertain. The choice of specifying a completely known source is also available.

Several design objectives are presented in this paper. Starting with the simplest one, the lining optimization for a given angular mode is done, as would be required for a tone. Next, the attenuation for the combination of all propagating modes, both circumferential and radial, at a given frequency is optimized. Finally, the broader objective of optimizing spectral attenuation is included in this study.

2. Liner design for tonal noise

This section considers explicitly the case of attenuation of pure tones. The model is a high by-pass turbofan engine with sub-sonic tip speed in which the choice of blade and vane count eliminates propagation of blade passage frequency. In the case chosen, the tone at twice blade passage frequency is investigated.

Details of scale model tests of the inlet for the Pratt & Whitney Advanced Ducted Propulsor (ADP) engine are available in Ref. [2]. A total of 18 blades and 45 fan exit guide vanes make the second blade passage frequency ($2\times$ BPF) harmonic dominant in the $m=-9$ circumferential mode [13]. The attenuation of this tone was chosen to be improved by optimizing the impedance. The approach (with Mach number $M=-0.288$) and cut-back ($M=-0.416$) flight conditions were considered. The dimensional and non-dimensional frequencies f and η_r for $2\times$ BPF were calculated as follows:

$$f=\mathrm{RPM}\,N_{\mathrm{blades}}\,N_{\mathrm{BPF}}, \tag{1}$$

$$\eta_r=\frac{2\pi fR}{c}, \tag{2}$$

where RPM for the model scale test rig is 5425 for approach and 8750 for cut-back, the number of blades $N_{\mathrm{blades}}=18$, the blade passage frequency harmonic $N_{\mathrm{BPF}}=2$, the model rig radius at the source $R=11.074$ in, and the speed of sound $c=1134$ ft/s for both approach and cut-back.

After using the above values in Eqs. (1) and (2) and with the knowledge that the engine is 5.91 larger than the model rig, the tonal frequencies for the engine were calculated to be: $f^{\mathrm{approach}}=550.8$ Hz, $f^{\mathrm{cutback}}=888.3$ Hz, or in non-dimensional form, $\eta_r^{\mathrm{approach}}=16.67$, $\eta_r^{\mathrm{cutback}}=26.89$, the same for both model scale and full scale engine. The duct geometry with a sample finite element mesh used is shown in Fig. 1.

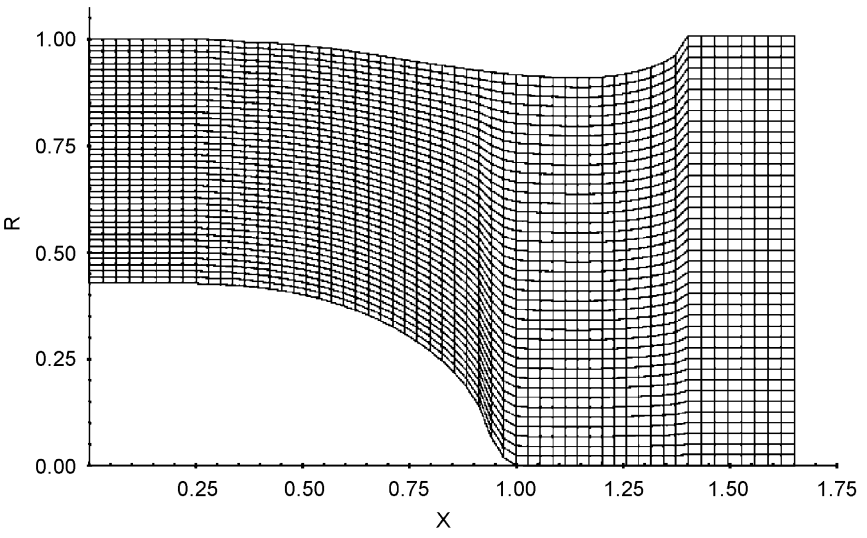

Fig. 1. ADP inlet geometry.

Table 1
Mean power attenuation for 2nd BPF at approach and cut-back, $m = -9$, ADP inlet

Frequency (Hz)	Lining 1	Lining 2	Lining 3	Optimum 1 23 elements	Optimum 2 12 + 11 elements	Optimum 3 8 + 8 + 7 elements
550.8 (approach)					2.22−0.31i	0.86−0.92i
	1.72−0.6i	2.34−1.81i	2.50−1.88i	2.42−0.79i	2.23−1.65i	Hardwall
						1.03−0.98i
	11.34 dB	11.24 dB	11.18 dB	12.19 dB	12.48 dB	19.96 dB
888.3 (cut-back)					3.60−1.03i	2.67−1.67i
	1.89−0.38i	2.58−0.79i	2.82−0.92i	3.30−0.54i	3.04−0.25i	4.15 + 1.16i
						2.84−0.73i
	3.85 dB	4.09 dB	4.12 dB	4.18 dB	4.19 dB	4.28 dB

1000 cases of random incident modal power and phases.

The duct profile is terminated by a section of uniform duct where the non-reflecting termination is enforced and where transmitted modal powers are computed. The mesh shown has 56 quadratic elements in the axial direction, and 40 elements in the radial direction, meeting the rule of thumb five quadratic three noded elements per wave length. In the axial direction wave length shortening due to local convection is accounted for. Higher frequencies later considered in the investigation required increased density meshes.

The outer wall lining starts from $x = 0.478$ (normalized with respect to R), and extends to $x = 1.145$ over 23 elements. The centerbody was not acoustically treated. It was assumed that the source was only known statistically, so 1000 cases of random modal power and phase were considered. The mean acoustic power attenuation was maximized. The rapid computational scheme based on a multiple input vector form of the frontal solver and an influence coefficient matrix, described in Ref. [6] was used to generate solutions to the many random sets of source data.

At the lower frequency, $\eta_r = 16.67$, there are only two cut-on modes propagating at the source plane. The higher frequency case, $\eta_r = 26.89$, has five propagating modes at the source. In the first optimization case, the impedance of the liner was assumed uniform. Next, the total lining length of $0.667R$ (23 elements) was maintained, but two sections of lengths $0.348R$ (12 elements) and $0.319R$ (11 elements), and ultimately three sections of lengths $0.232R$ (8 elements), $0.232R$ (8 elements) and $0.203R$ (7 elements) were allowed to have distinct impedances that were optimized. The results are shown in Table 1. For comparison, calculated mean attenuation performances for three NASA proposed linings are also presented [6]. The three linings are lining 1, the ''1992 single degree of freedom'', lining 2, the ''improved single degree of freedom'', and lining 3 is the ''double degree of freedom''.

For each frequency specified, impedances [6] and predicted mean attenuation are shown in the first three columns. Then three additional columns show impedances that optimize mean attenuation based on one, two, and three lining segments. Optimized attenuation is also shown for the optimum impedances. It can be seen that impedance segmentation can produce better attenuation values, however, this seems to be limited to the lower frequency case with only two propagating modes. It is interesting to observe that for three-segment optimization at 550.8 Hz approach frequency, the embedded hardwall section apparently produces scattered modes that the last section more easily attenuates. This emphasizes the fact that modal scattering can play an important role in realized attenuation. Attenuation maps are shown in Fig. 2. The locations of the impedances of the three linings relative to the optimum are also marked. It is shown that at approach, Lining 1 with a reactance closer to the optimum (single segment) than that of the other two linings performs best, although the attenuation differences are small. At cut-back, Lining 3 achieves the best attenuation out of the three tested, with its resistance closer to the optimum.

As noted, in this analysis it has been assumed that source modal power and phase are random, and the mean attenuation is maximized. However, there is available test data with respect to the source modal content. It is based on a list of hard wall cut-on modal amplitudes measured at the throat of the outer wall. A comparison of the optimum impedances between the random source model and the real, known source can be made. Since

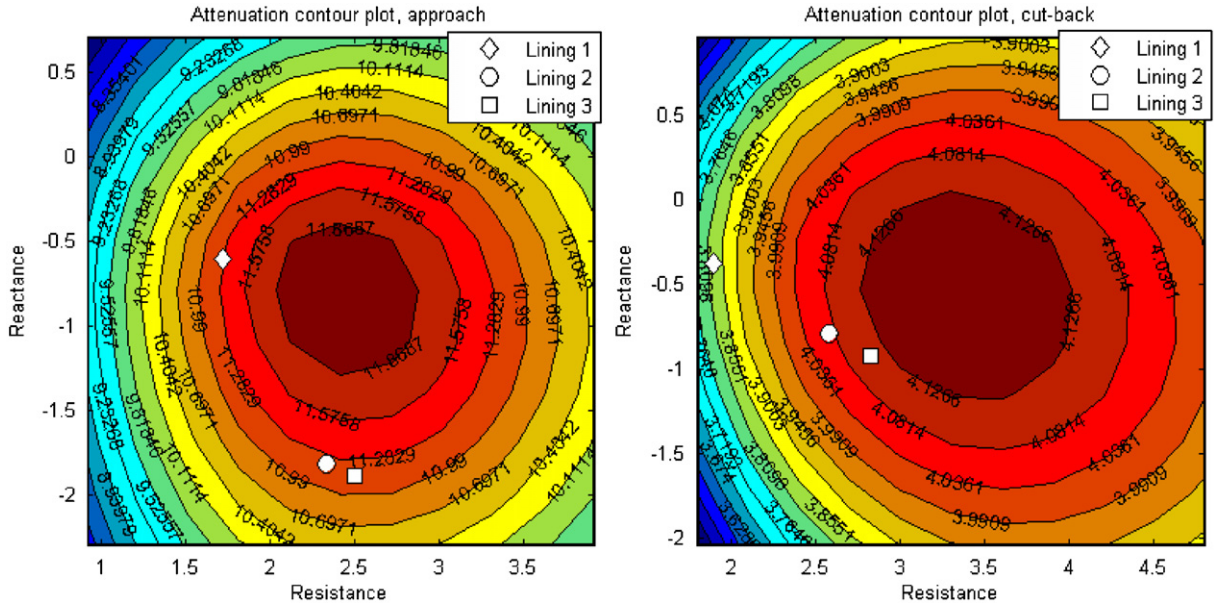

Fig. 2. Mean attenuation contour maps for 2nd BPF at approach and cut-back, $m = -9$, ADP inlet, using the random modal source model: ◇ lining 1 impedence; ○ lining 2 impedence; □ lining 3 impedence.

Table 2
Power attenuation for 2nd BPF at approach and cutback, $m = -9$, ADP inlet, using determined incident modal power and phases

Frequency (Hz)	Lining 1	Lining 2	Lining 3	Optimum 1 23 elements	Optimum 2 12 + 11 elements	Optimum 3 8 + 8 + 7 elements
550.8 (approach)					Hardwall	Hardwall
	1.72−0.6i	2.34−1.81i	2.50−1.88i	3.56−0.91i	1.80−0.70i	Hardwall 0.11−0.83i
	7.47 dB	8.85 dB	9.09 dB	10.60 dB	19.28 dB	25.35 dB
888.3 (cut-back)					6.37−0.75i	4.22−3.08i
	1.89−0.38i	2.58−0.79i	2.82−0.92i	3.69−0.62i	2.17−0.81i	3.31 + 0.53i 1.26−1.28i
	3.98 dB	4.38 dB	4.45 dB	4.57 dB	4.74 dB	4.70 dB

modal amplitudes at the source section are needed as input for the propagation code, a separate procedure was used to determine them from the values read experimentally at the throat.

Table 2 shows the attenuation results for the approach and cut-back flight conditions using the determined incident modal amplitudes. Once more, the nominal lining is assumed to begin at $x = 0.478R$ and has of total length of $0.667R$. For approach, it can be observed that hardwall sections result as optimum for the first or first two sections of the segmented liners, meaning that a shorter lining suitably placed can be optimum. For Optimum 3, 7 lined elements (length $0.203R$), correctly positioned, in this case, toward the duct throat, deliver a better acoustic attenuation than 23 elements ($0.667R$) as in the Optimum 1 case. It is shown in Table 2 Optimum 3 at cut-back has converged to a slightly lower optimum attenuation value than Optimum 2; however, this does not necessarily imply that perhaps a local optimum was found (as opposed to a global optimum). Note that the segmentation of Optimum 3 cannot match that of Optimum 2 due to the unequal lengths. The only conclusion is that there is little difference between Optimum 2 and 3.

If optimum impedance values in Tables 1 and 2 are compared, even though they are not the same, the optimum liner obtained as a result of optimizing the mean attenuation, statistically has a good chance of achieving a useful attenuation with a large range of potential modal amplitudes, including the actual ones.

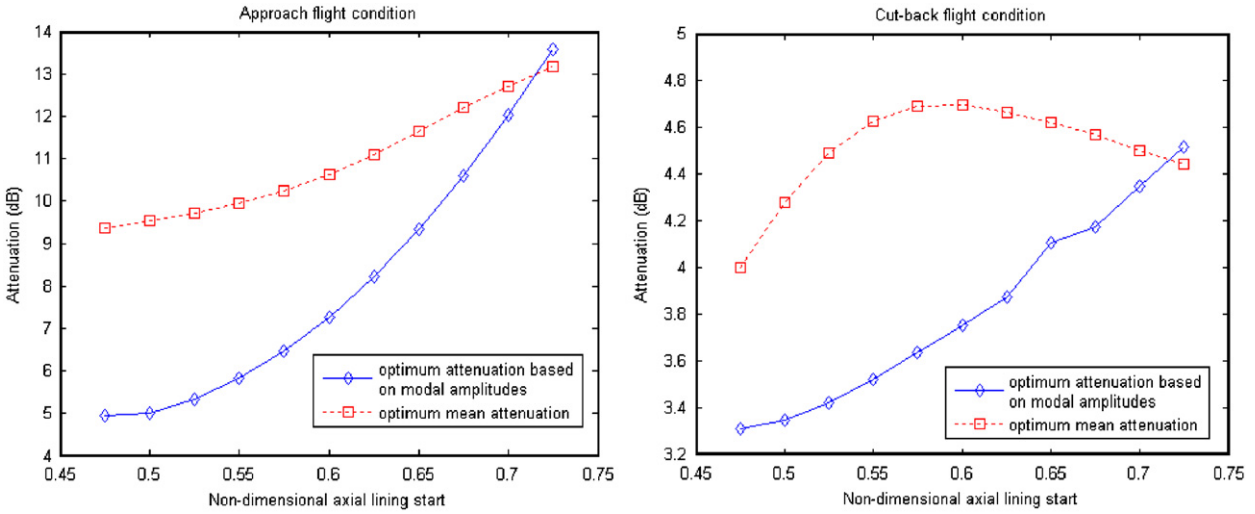

Fig. 3. Optimum mean and measured mode amplitude based attenuation variations with lining position for 2nd BPF at approach and cut-back (mode $m = -9$), ADP inlet: —◇— optimum attenuation based on modal amplitudes; - - -□- - - optimum mean attenuation.

The segmented liner results in Table 2 suggest that positioning of the liner can be an important factor in liner performance, at least when few modes propagate. The present study does not simultaneously vary lining position and impedance in the optimization search. However, it is possible to examine the effect of position on a lining of given length and impedance. In Fig. 3, the optimum single segment lining for the ADP example of Tables 1 and 2 is repositioned from the nominal position (but impedance remains optimum for the nominal position).

It is found that optimum attenuation varies significantly with the lining axial position. The mean attenuation has a lower degree of variation than the attenuation provided by the actual modal amplitudes. Any potential attenuation improvement diminishes with the increase in frequency and this is in direct connection with the presence of an increased number of incident source modes. The study has found that, generally, lining positions that perform well are the ones that are in the vicinity of the throat. Best lining position, as well as optimum impedance will vary with frequency and mean flow.

3. Liner design for broadband noise

At high tip speeds, tone noise dominates the noise levels of turbofan engines. As tip speeds are lowered, the relative strengths of tone and broadband noise change so that broadband noise becomes increasingly dominant. Broadband noise analysis, as opposed to tonal noise, entails taking into account a range of frequencies. At each frequency all circumferential and radial propagating modes are considered. The ADP engine was studied at both cut-back and approach in a 250–4000 Hz frequency range.

Broadband noise has an inherently random character. In this study the source at a given frequency is represented by all propagating circumferential and radial modes. Sets of 1000 random modal inputs are considered sufficient to provide an accurate mean attenuation. In the hardwall source and termination duct sections radial and angular modal powers for propagating incident, transmitted and reflected powers can be summed and an overall power attenuation can be calculated for the set of all modes propagating at 1/3 octave band center frequencies. The resulting sets of 1000 attenuations have a stable statistical distribution [7] from which the mean attenuation is determined and optimized. The purpose is to determine the impedance at each 1/3 octave band center frequency of a lining that has the best chance, statistically speaking, to attenuate a random noise source.

For the ADP inlet, the optimum mean attenuation levels and the corresponding optimum impedances varying with frequency are shown in Fig. 4 for approach and cut-back. Note that optimums are for each 1/3 octave band center frequency, and therefore, represent different lining parameters such as open area and

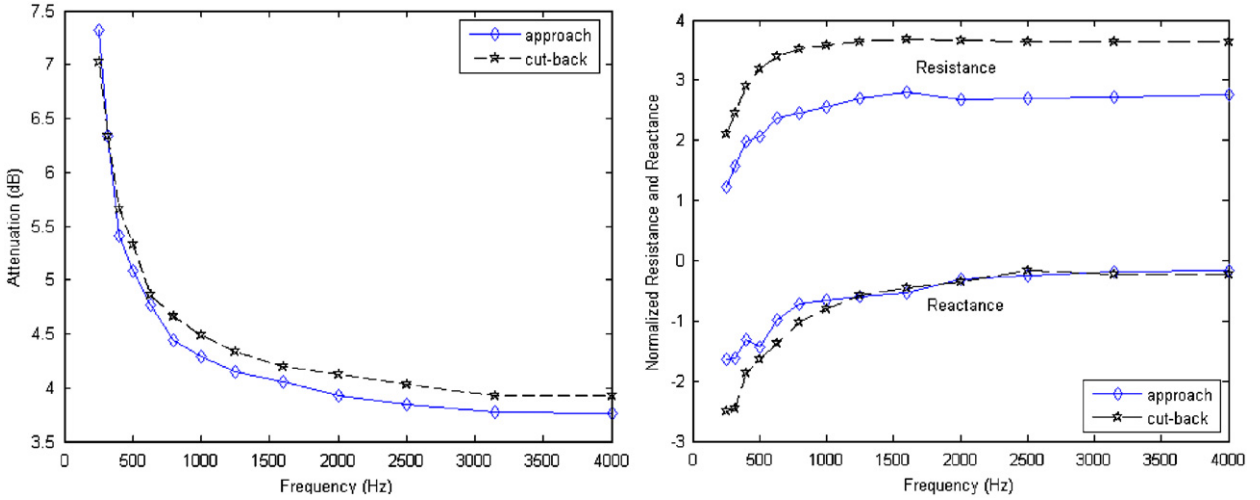

Fig. 4. Broadband noise optimum mean attenuation and the corresponding optimum impedance for third octave band center frequencies in the 250–4000 Hz range for the ADP inlet: —◇— approach; —☆— cut-back.

backing space depth. A single choice of open area and backing depth would be optimum for just one frequency.

The value of the broadband noise optimum mean attenuation for approach and cut-back starts at around 7 dB for 250 Hz and decreases with frequency, remaining at between 3.5 and 4 dB at the higher frequencies. It can be seen that the optimum mean attenuation for the cut-back flight condition is higher throughout most of the spectrum, except for the lowest frequencies, 250 and 315 Hz. The difference between the cut-back and approach optimum attenuations is small, and it does not exceed 0.3 dB. Optimum resistance increases with frequency and tends to normalized values around 3.6 and 2.7 for frequencies over 1000 Hz for approach and cut-back, respectively. The optimum reactance also stabilizes for higher frequencies at small negative values for both approach and cut-back.

Equal mean attenuation contours in the impedance plane, as shown in Fig. 5, give a better understanding of the effect of shift from optimum values of both reactance and resistance in case of actual linings. Starting with the lowest frequency of 250 Hz, resistances lower than the optimum would produce a more pronounced mean attenuation drop than a resistance that exceeds the optimum. This tendency becomes more obvious with increase in frequency, and has been observed at all considered frequencies for both approach and cut-back flight conditions. The trend has been observed to take place even in the case of tonal noise, as Fig. 2 showed. Reactance that deviates from the optimum values does not have a definite favorable direction in which the attenuation drop is less pronounced, even though the higher frequencies seem to show a steeper attenuation drop for higher than optimum resistance.

The performance of Linings 1, 2 and 3 was compared to the corresponding optimums. First, a direct comparison for the resistance of the three linings, from available impedance data from the ADP program, and the optimum resistance is shown in Fig. 6 for both approach and cut-back at all the frequencies in the 250–4000 Hz range. Data shows the resistance of Linings 1 and 2 to depend on Mach number but not frequency. Lining 3 has resistance dependent on Mach number and frequency. It can be seen that Linings 1 and 2 have lower resistances than the optimum at both cut-back and approach in the high frequency range. This fact will most likely affect adversely attenuation at high frequencies for these two linings. Lining 3 has throughout a higher resistance than the optimum at approach, but it is lower at cut-back. Nevertheless it is closer to the optimum than the resistance of the other two linings.

The values of the reactance for Linings 1, 2 and 3 do not change with the mean flow Mach number, but depend on frequency. Their values are compared with the optimum ones for both approach and cut-back in Fig. 7. The presence of resonance in the reactance variation with frequency is obvious in Fig. 7 for both Lining 1 and 2. These discontinuities separate the actual impedance from the optimum values, resulting in reduced

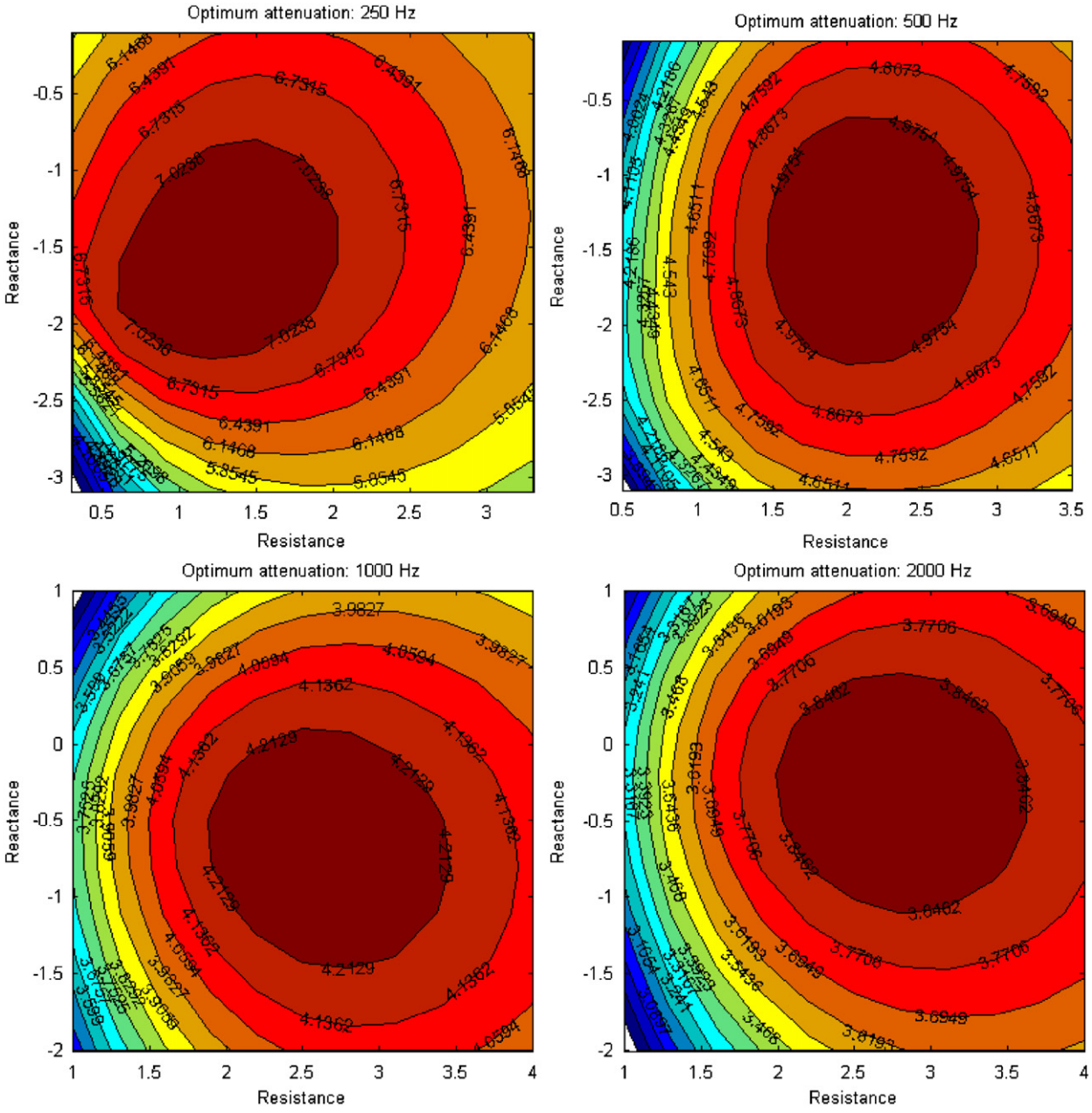

Fig. 5. Mean attenuation maps for several frequencies at approach, for the ADP inlet. Upper left 250 Hz, upper right 500 Hz, lower left 1000 Hz, lower right 2000 Hz.

attenuation. The mean attenuations achieved by Linings 1, 2 and 3 compared with the optimum ones throughout all frequencies in the spectrum can be seen in Fig. 8. The large number of randomly powered and phased acoustic sources appears to render the achievable attenuation relatively insensitive to frequency, except at low frequencies where the mode count is relatively low.

For both cut-back and approach, the mean attenuation of Lining 1 stays close to the optimum for the lowest three frequencies, but as the frequency increases, its performance deteriorates, with the largest deviations at 2000 and 4000 Hz, where the largest deviation of reactance from optimum to occurs. Lining 2 has a better performance than Lining 1, but after 2000 Hz the deviation of reactance from optimum in addition to

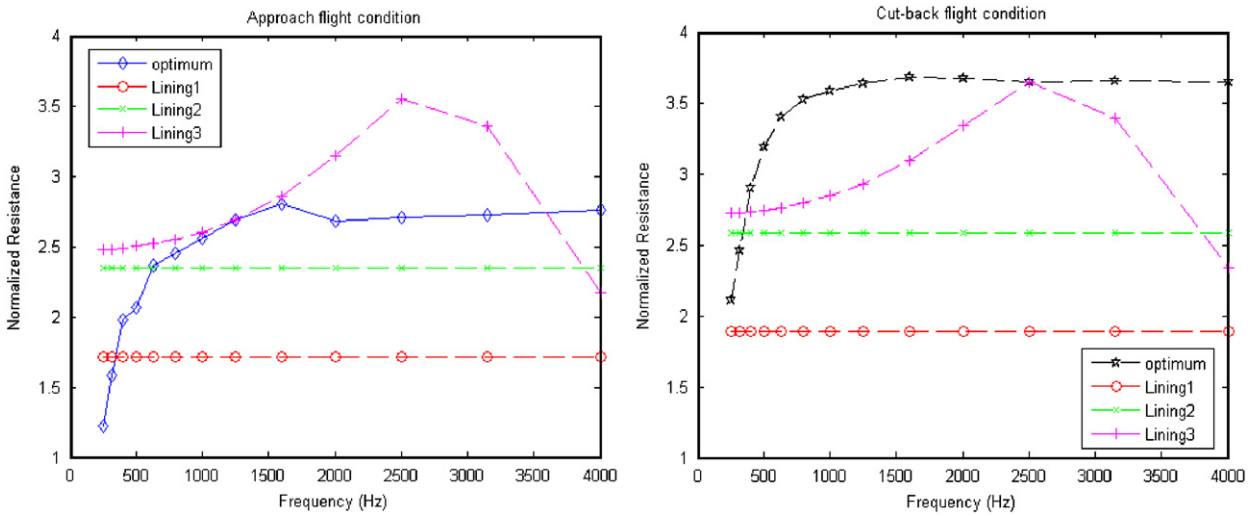

Fig. 6. Comparison between optimum resistance and the resistance of Linings 1, 2, 3. Approach, left, cut-back right. —◇— optimum resistance at approach; —☆— optimum resistance at cut-back; —○— resistance of lining 1; —×— resistance of lining 2; —+— resistance of lining 3.

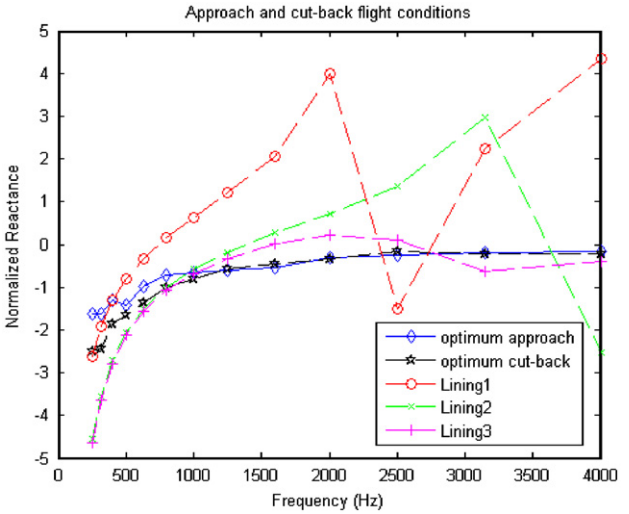

Fig. 7. Comparison between optimum reactance and the reactance of Linings 1, 2, 3: —◇— optimum reactance at approach; —☆— optimum reactance at cut-back; —○— reactance of lining 1; —×— reactance of lining 2; —+— reactance of lining 3.

a lower resistance than the optimum, causes a drop in attenuation. Lining 3, a two degree of freedom lining, has its resistance as well as reactance close to the optimum values and this is why it attenuates very well throughout the spectrum, except for the lowest two frequencies where both resistance and reactance deviate from optimum.

In Tables 3 and 4 are given the optimum impedances of uniform linings throughout the spectrum with optimized two- and three-segment linings for approach and cut-back, respectively. The corresponding mean attenuation values are also shown. It can be noted that for two segment optimum linings, with a few exceptions in the low frequencies, the two optimum resistances and reactances bracket the optimum resistance and reactance of the uniform lining, with the first segment having a lower resistance and reactance closer to zero. A similar result can be observed for the three-segment optimum lining results.

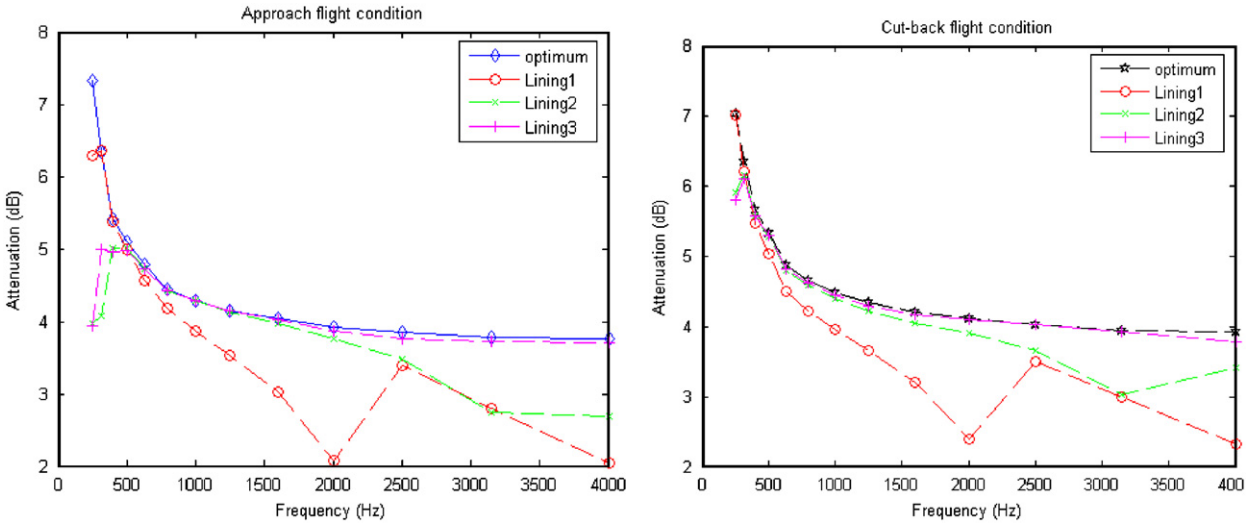

Fig. 8. Attenuation comparison between optimum and Linings 1, 2, 3: —◇— optimum attenuation at approach; —☆— optimum attenuation at cut-back; —○— attenuation of lining 1; —×— attenuation of lining 2; —|— attenuation of lining 3.

In Table 2 it has been shown previously that for tonal noise, multi-segmented optimized linings can generate increased mean attenuation compared to a uniform impedance optimum lining, especially in the cases of low frequencies. This occurs too for broadband noise, as results in Tables 3 and 4 illustrate, though not so dramatically as for the cut-back case of tonal noise.

The mean attenuation gains that would be achieved by a two- and three-segment lining, compared to a similarly long uniform lining are shown in Fig. 9 for both approach and cut-back. It can be seen that broadband noise attenuation gain produced by segmented optimum lining is minimal for higher frequencies.

When using the statistical approach for optimization of liners for broadband noise, the mean attenuation is the objective function. This of course is not the most conservative approach. Although, as shown in Ref. [6], standard deviation tends to be small, there is the chance of missing the target attenuation. Another option would be to maximize, more conservatively, the minimum value in the attenuation range.

In order to obtain reliable mean attenuation, the authors have shown that 1000 samples of modal power and phase distributions are sufficient to determine a stable mean [6]. On the other hand, extreme values in the achievable range are less reliable and sizeable sample sets are required for accuracy. In the present optimization process, the size of incident random modal source being limited to 1000, optimizing the acoustic liner to raise the minimum achievable attenuation is an exercise only meant to provide a general comparison basis for optimum impedances, with no claim of perfect accuracy. The results of this comparison are presented in Fig. 10. The results lead to much less smooth curves for optimum impedance, symptomatic of the small sample space. However, the results are similar enough to the results of optimization of the mean attenuation, that a meaningful conclusion can be drawn. In Refs. [6,7] the authors discuss statistical analysis with as many as 100,000 random trials.

The optimum impedance values for both approach and cut-back are nearly the same for the mean and the minimum attenuation. Consequently, optimizing the impedance by maximizing either the mean attenuation or the minimum attenuation yields similar results.

4. Attenuation spectrum optimization

The task of designing a liner that would respond well to broad-band noise at all frequencies in a chosen range will be carried out next for both approach and cut-back. In this analysis a single-degree-of-freedom (sdof) liner consisting of perforate sheet attached to a honeycomb back cavity structure will be considered for optimization. A theoretical model proposed by Heidelberg and Rice [14] defines the resistance of the non-

Table 3
Optimum impedances and mean attenuations for one, two and three segment linings at approach

Frequency (Hz)	Optimum 1 segment lining		Optimum 2 segment lining		Optimum 3 segment lining	
	Atten (dB)	Impedance	Atten (dB)	Impedance	Atten (dB)	Impedance
250	7.031	2.11−2.49i	7.228	1.54−1.30i 1.85−3.68i	7.720	0.68−1.70i Hard wall 1.89−2.91i
315	6.337	2.46−2.45i	6.358	2.03−2.38i 2.99−2.45i	6.713	0.91−1.91i Hard wall 1.54−2.17i
400	5.656	2.90−1.86i	5.682	2.66−1.13i 2.93−2.52i	6.175	1.64−1.71i Hard wall 1.53−2.41i
500	5.331	3.18−1.64i	5.337	2.91−1.73i 3.43−1.55i	5.589	1.31−2.09i Hard wall 1.72−1.78i
630	4.867	3.40−1.36i	4.879	3.05−1.27i 3.73−1.47i	5.039	2.19−1.83i 6.22+1.82i 2.64−2.08i
800	4.663	3.52−1.02i	4.669	3.38−1.19i 3.55−0.79i	4.767	2.62−1.71i 4.70+1.21i 3.09−1.77i
1000	4.490	3.58−0.79i	4.492	3.40−0.83i 3.73−0.74i	4.548	3.00−1.48i 4.05+0.70i 3.39−1.46i
1250	4.339	3.64−0.57i	4.341	3.44−0.55i 0.83−0.60i	4.371	3.26−1.08i 3.86+0.45i 3.69−1.18i
1600	4.197	3.68−0.45i	4.199	3.49−0.43i 3.87−0.46i	4.215	3.35−0.79i 3.87+0.26i 3.79−0.89i
2000	4.123	3.67−0.35i	4.124	3.50−0.34i 3.82−0.35i	4.135	3.38−0.63i 3.80+0.18i 3.82−0.69i
2500	4.030	3.64−0.16i	4.031	3.53−0.28i 3.82−0.27i	4.039	3.45−0.50i 3.75+0.14i 3.8−0.55i
3150	3.923	3.65−0.23i	3.930	3.57−0.24i 3.74−0.22i	3.934	3.48−0.41i 3.73+0.08i 3.70−0.40i
4000	3.927	3.64−0.22i	3.928	3.62−0.21i 3.66−0.24i	3.931	3.53−0.35i 3.74+0.08i 3.64−0.40i

dimensional impedance $Z = R + \mathrm{i}X$ as

$$R = \frac{M}{\sigma\left(2 + 1.256(\delta/d)\right)}, \tag{3}$$

where M is the mean flow Mach number, σ is the face sheet open area ratio, δ is the boundary layer displacement thickness and d the diameter of the holes in the perforate face sheet.

Table 4
Optimum impedances and mean attenuations for one, two and three segment linings at cut-back

Frequency (Hz)	Optimum 1 segment lining		Optimum 2 segment lining		Optimum 3 segment lining	
	Atten (dB)	Impedance	Atten (dB)	Impedance	Atten (dB)	Impedance
250	7.321	1.23−1.64i	7.497	1.20−0.73i 0.87−2.08i	7.975	0.63−0.99i Hard wall 0.55−1.70i
315	6.358	1.58−1.61i	6.405	1.28−1.38i 1.93−2.08i	6.767	0.66−1.22i Hard wall 0.96−1.62i
400	5.410	1.98−1.31i	5.432	1.93−0.79i 1.89−1.73i	6.115	0.98−1.05i Hard wall 0.89−1.50i
500	5.089	2.07−1.43i	5.103	1.81−1.32i 2.33−1.52i	5.444	1.04−1.35i Hard wall 1.19−1.53i
630	4.772	2.37−0.98i	4.781	2.16−0.73i 2.49−1.28i	4.994	1.50−1.37i 3.90+3.32i 1.44−1.68i
800	4.439	2.45−0.72i	4.445	2.29−0.55i 2.65−0.99i	4.559	1.85−1.14i 3.35+1.36i 1.88−1.58i
1000	4.293	2.56−0.66i	4.297	2.36−0.53i 2.73−0.76i	4.357	2.09−0.97i 3.10+0.57i 2.27−1.34i
1250	4.153	2.69−0.59i	4.157	2.49−0.42i 2.77−0.58i	4.195	2.31−0.79i 2.89+0.38i 2.51−1.10i
1600	4.052	2.80−0.53i	4.059	2.52−0.32i 2.84−0.44i	4.080	2.40−0.58i 2.82+0.23i 2.71−0.88i
2000	3.925	2.68−0.30i	3.927	2.57−0.11i 2.76−0.44i	3.940	2.45−0.43i 2.81+0.13i 2.78−0.68i
2500	3.849	2.70−0.24i	3.852	2.55−0.19i 2.97−0.29i	3.860	2.49−0.33i 2.76+0.10i 2.84−0.57i
3150	3.778	2.73−0.20i	3.780	2.60−0.17i 2.85−0.23i	3.785	2.55−0.28i 2.78+0.06i 2.86−0.44i
4000	3.758	2.76−0.17i	3.759	2.67−0.14i 2.85−0.20i	3.763	2.58−0.24i 2.84+0.05i 2.84−0.36i

The same model proposes for reactance the expression

$$X = \frac{2\pi\tau}{\sigma\lambda} - \cot\left(\frac{2\pi h}{\lambda}\right), \tag{4}$$

where τ is the face sheet thickness, λ the acoustic wave length, and h the depth of the honeycomb cavity.

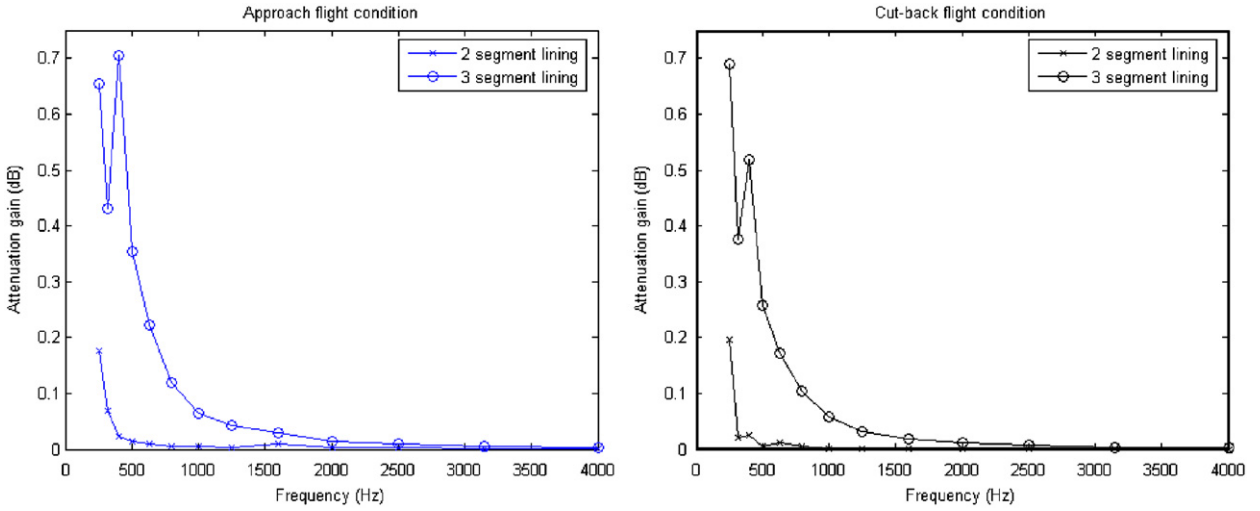

Fig. 9. Mean attenuation gains of two- and three-segment optimized linings compared to an optimum uniform lining. Approach, left, cut-back right. —×— 2 segment attenuation gain, approach; —○— 3 segment attenuation gain, approach; —×— 2 segment attenuation gain, cut-back; —○— 3 segment attenuation gain, cut-back.

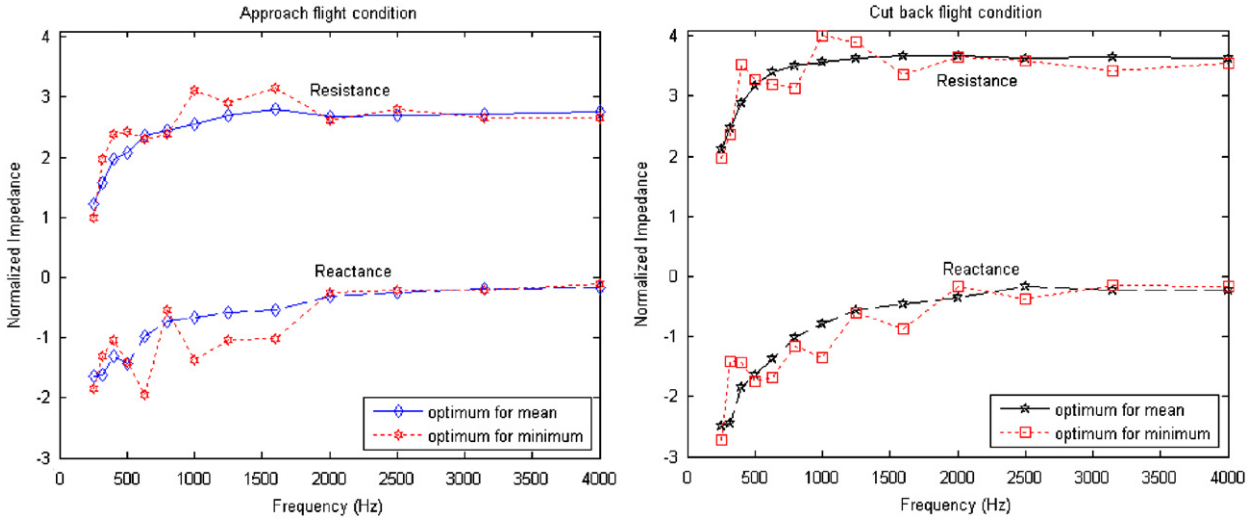

Fig. 10. Optimum impedance comparison: maximizing the mean and minimum attenuations. Approach, left, cut-back right. —◇— optimum for mean at approach; - - -☆- - - optimum for minimum at approach; —★— optimum for mean at cut-back; - - -□- - - optimum for minimum at cut-back.

Of the parameters present in Eqs. (3) and (4), the flow Mach number is specified, and wave length depending on frequency can be calculated. Structural reasons may dictate the thickness of the perforated plate and ratio of boundary layer thickness to hole diameter may not be fully controllable. It is therefore considered that open area ratio and backing space depth are parameters to be optimized. In this investigation, a sheet thickness of 0.02 in (0.508 mm) and hole diameter of 0.05 in (1.27 mm) were chosen. The boundary layer thickness was approximated at 0.03 in (0.762 mm).

The face sheet porosity and the cavity backing depth were the lining characteristics selected to be the design objectives. Once more, sets of random modal power and phase characterize the random acoustic source. In the absence of spectral data, the acoustic source is assumed to generate pink noise, with equal power in each 1/3 octave band. Mean attenuation is calculated at the center frequency for each 1/3 octave band in the range

250–4000 Hz, and is taken to be power per unit band width (power spectrum), constant for the band. Power in the band is then the power per unit band width multiplied by the band width. In each band, all circumferential and radial propagating modes are considered with random power and random phase. In each 1/3 octave the modal powers are scaled to achieve equal power for all bands. Transmitted power at each 1/3 octave band center frequency is treated similarly, though of course without scaling. The transmitted powers in each third octave band are then noy weighted to simulate a simplified version of optimization of Perceived Noise Level. The powers in all third octave bands are calculated and then summed for both incident and transmitted acoustic power. The sheet open area ratio and cavity backing space depth are optimized with the objective function the noy weighted mean attenuation obtained for the whole spectrum considered. The cavity depth was not constrained. Results show that for approach, to obtain an optimal mean attenuation of 4.45 dB in the 250–4000 Hz spectrum, the perforate sheet should have an open area of 4.6% and the backing space should be 3.7 in (93.98 mm).

An interesting aspect of the liner broad-band noise optimization process is the presence of multiple local optimal values for the open area ratio, honeycomb depth pair, as can be observed in Fig. 11. In addition to the calculated 3.7 in (93.97 mm) optimal value for the depth of the honeycomb cavity, there are secondary values that generate local noy weighted maximums near 2.5 or 5 in (63.50 or 127 mm). The optimal open area ratio does not seem to change. For structural and weight reasons if backing depth near 3.7 in (93.98 mm) is not acceptable, the optimization can be constrained to smaller values and another local optimum with lower core depth can be chosen.

Another feature revealed by Fig. 11 is the relative flatness of the mean attenuation contour plot, which means that even if the optimal porosity and backing space depth are not achieved, still the overall spectral mean attenuation is not far from the maximum value achievable. The spectral optimum impedance values at the third octave band center frequencies generated from the optimal backing space depth and porosity by using Eqs. (3) and (4), are shown in Fig. 12 and for comparison purposes the optimum impedances at each center frequency are also plotted. At approach, the optimal resistance for the spectrum is 2.8, which is very close to the optimum resistance for frequencies over 1000 Hz, seen previously to be around the value of 2.7. The reactance starts from low negative values and intersects the optimum reactance for the 1600 Hz frequency, passing then to positive values and achieving the first discontinuity over 5000 Hz (not shown on the graph).

It should be mentioned that in building the FEM mesh, the rule of thumb of 5 quadratic elements per distance equal to one wave length made the mesh mentioned previously (56 elements in the axial direction and 40 in the radial direction) suitable up to the 1000 Hz frequency. For frequencies over 1000 Hz and up to 2000 Hz, the mesh density was doubled in both axial and radial directions. Over 2000 Hz, the mesh density should have been doubled once more in both directions, resulting in prohibitive execution times for the

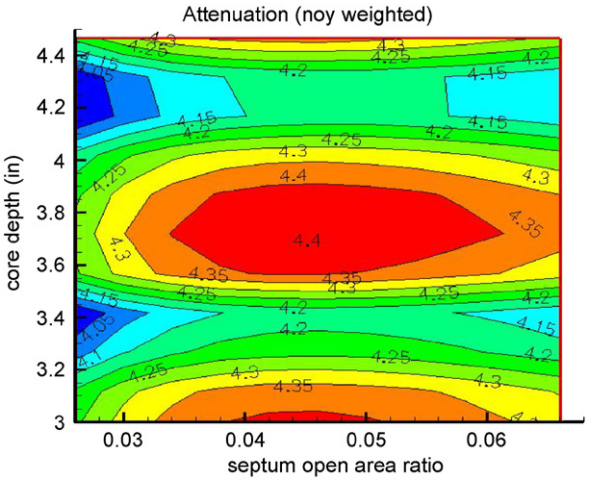

Fig. 11. Broad-band noise overall noy weighted mean attenuation contour maps for the 250–4000 Hz frequency rage, ADP engine at approach.

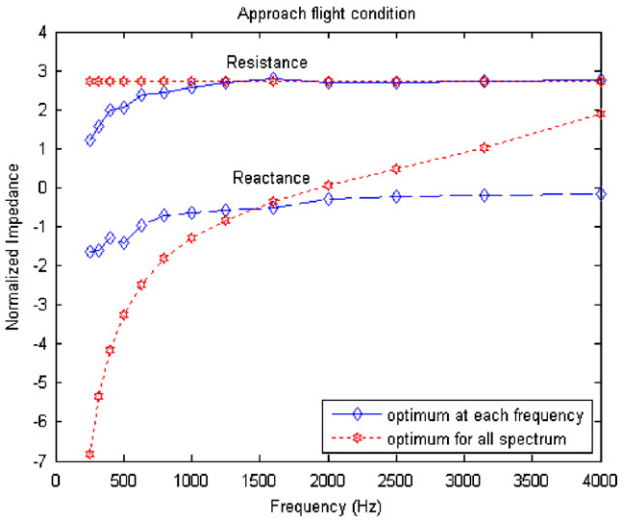

Fig. 12. Optimum spectrum impedance comparison with optimum impedances at each 3rd octave band central frequencies: —◇— optimum at each frequency; - - -☆- - - optimum for all spectrum.

purpose of this study. This was not done for reasons of efficiency because experience has shown that metrics such as attenuation are far less sensitive to mesh resolution than details such as local acoustic pressure.

5. Conclusions

A new method for representation of a statistically defined source has been applied in the design process of turbofan inlet liners. This is an alternative to the standard approach in which more is assumed about the details of the source than is realistically available. Many trials of sets of random modal power and random modal phase are used to characterize a broadband noise source or an ill-defined tonal source. With an efficient propagation model a statistical description of attenuation is generated. The method is integrated in a finite element formulation for propagation in a non-uniform duct with compressible potential mean flow. A repeatable mean value for attenuation results, and is maximized in the optimization process.

Three examples of lining design have been presented. In the simplest case, acoustic treatment is optimized for tonal noise in which the circumferential mode is known. In the second case broadband noise is considered and all propagating circumferential and radial modes are considered. The optimum impedance is determined for each 1/3 octave band center frequency between 250 and 4000 Hz. This leads to a different lining (in terms of open area fraction and backing depth, for example) for each frequency. Finally, a single lining is optimized to achieve maximum noy weighted attenuation for an initially pink noise spectrum source.

In the course of the investigation, for low frequency tonal noise with few propagating modes, there is seen the possible advantage of a segmented liner with two or three different impedances, as compared to a uniform liner of the same length. In the same case lining position relative to the source is also found to be a parameter in lining performance. It is shown in one case that with proper placement the length of acoustic treatment can be reduced for a target attenuation.

The optimization process reveals that for broadband noise attenuation is relatively insensitive to slight variations of impedance relative to the optimum. If resistance close to the optimum cannot be achieved in a design process that targets certain frequencies from the broad-band noise spectrum, it has been shown consistently that over prediction of resistance will yield less negative effect on attenuation than under prediction. In the cases of broadband noise studied, it is concluded linings for which resistance is constant throughout the frequency spectrum should target resistance values close to the optimum in the high frequencies.

In comparison with data available from published experiments, it is clear that a reported two degree of freedom lining does a much better job of emulation of the optimum impedance at all frequencies in the

spectrum. Comparisons of predicted optimum linings with other tested single degree of freedom linings reveal that performance degradation is traced to deviations of resistance and reactance from the optimum values.

The proposed statistical approach to impedance optimization has been shown to be a viable alternative to conventional design procedures that assume an optimistic level of knowledge of source details. The statistical method accepts uncertainty in the source model and provides statistically based metrics of performance.

References

[1] H. Lester, J.W. Posey, Duct liner optimization for turbomachinery noise sources, *NASA TM X-72789* (1975).
[2] G.W. Bielak, J.W. Premo, A.S. Hersh, Advanced turbofan duct liner concepts, *NASA CR 209002* (1999).
[3] J.H. Lan, Turbofan duct propagation model, *NASA CR 211245* (2001).
[4] I. Dyer, Measurement of noise sources in ducts, *Journal of Acoustical Society of America* 30 (1958) 833–841.
[5] G. Zlavog, W. Eversman, Source effects on realized attenuation in lined ducts, AIAA paper 2003-3247, 2003.
[6] G. Zlavog, W. Eversman, Source effects on attenuation in lined ducts. Part I: A statistically based computational approach,, *Journal of Sound and Vibration* 307 (2007) 113–138.
[7] G. Zlavog, W. Eversman, Source effects on attenuation in lined ducts. Part II: statistical properties,, *Journal of Sound and Vibration* 307 (2007) 139–151.
[8] L. Lafronza, A. Mc.Alpine, A.J. Keane, R.J. Astley, Computer aided liner optimization for broadband noise, AIAA paper 2004-3029, 2004.
[9] W. Eversman, A reverse flow theorem and acoustic reciprocity in compressible potential flow in ducts, *Journal of Sound and Vibration* 246 (1) (2001) 71–95.
[10] W. Eversman, Numerical experiments on acoustic reciprocity in compressible potential flows in ducts, *Journal of Sound and Vibration* 246 (1) (2002) 97–113.
[11] C.L. Morfey, Acoustic energy in non-uniform flows, *Journal of Sound and Vibration* (1971) 159–170.
[12] J.A. Nelder, R. Mead, A simplex method for function minimization, *Computer Journal* 7 (1965) 308–313.
[13] J.M. Tyler, T.G. Sofrin, Axial flow compressor noise studies, *SAE Transactions* 70 (1962) 309–332.
[14] L.J. Heidelberg, L.J. Rice, L. Homyak, Experimental evaluation of a spinning-mode acoustic-treatment design concept for aircraft inlets, *NASA TP* 1613 (1980).